Efficacy of Utilizing Both 3-Dimensional Multimodal Fusion Image and Intra-Arterial Indocyanine Green Videoangiography in Cerebral Arteriovenous Malformation Surgery

Kenji Shimada, Kazuhisa Miyake, Izumi Yamaguchi, Shu Sogabe, Masaaki Korai, Yasuhisa Kanematsu, Yasushi Takagi

■ OBJECTIVE: **An understanding of the complex morphology of an arteriovenous malformation (AVM) is important for successful resection. We have previously reported the utility of intra-arterial indocyanine green (ICG) videoangiography for this purpose, but that method cannot detect the angioarchitecture covered by brain tissue. 3-dimensional (3D) multimodal fusion imaging is reportedly useful for this same purpose, but cannot always visualize the exact angioarchitecture due to poor source images and processing techniques. This study examined the results of utilizing both techniques in patients with AVMs.**

■ METHODS: **Both techniques were applied in 12 patients with AVMs. Both images were compared with surgical views and evaluated by surgeons.**

■ RESULTS: **Although evaluations for identifying superficial feeders by ICG videoangiography were high in all cases, the more complicated the AVM, the lower the evaluation by 3D multimodal fusion imaging. Conversely, evaluation of the estimated range of the nidus was high in all cases by 3D multimodal fusion imaging, but low in all but one case by ICG videoangiography. Nidus flow reduction was recognized by Flow 800 analysis obtained after ICG videoangiography.**

■ CONCLUSIONS: **These results showed that utilizing both techniques together was more useful than each modality alone in AVM surgery. This was particularly effective in identifying superficial feeders and estimating the range of the nidus. This technique is expected to offer an optimal tool for AVM surgery.**

INTRODUCTION

Indocyanine green (ICG) videoangiography is a frequently used intraoperative technique for vascular neurosurgeries like cerebral aneurysm treatment, extracranial-intracranial bypass, and arteriovenous malformation (AVM) surgery. In AVM surgery, an understanding of the angioarchitecture is crucial for successful resection. However, in cases examined under intravenous ICG videoangiography, ICG remains in vessels during the late phase, presenting an obstacle to understanding the vascular anatomy. In addition, because of the large amount of ICG required to reach the intracranial arteries due to dilution in the cardiopulmonary circulation, a long washout time is required to remove the ICG. We have previously reported the utility of intra-arterial ICG videoangiography in neurosurgical procedures.[1,2] This technique can be added to intraoperative digital subtraction angiography (DSA) without time-consuming processing, and can be repeated within a short period due to the short ICG washout time, unlike intravenous ICG videoangiography.[1] This method is useful for differentiating between feeders and drainers, due to the bright, high phase contrast and for confirming reduced nidus flow or

Key words
- 3D multimodal fusion image
- Cerebral arteriovenous malformation
- Drainer
- Feeder
- Intra-arterial ICG videoangiography
- Nidus

Abbreviations and Acronyms
3D: Three-dimensional
3DRA: Three-dimensional rotational angiography
AVM: Arteriovenous malformation
CT: Computed tomography
DSA: Digital subtraction angiography
ICG: Indocyanine green
MRI: Magnetic resonance imaging
PICA: Posterior inferior cerebellar artery
SCA: Superior cerebellar artery
SPGR: Spoiled gradient echo
T1WI: T1-weighted imaging

Department of Neurosurgery, Tokushima University, Tokushima, Tokushima, Japan

To whom correspondence should be addressed: Kenji Shimada, M.D., Ph.D. [E-mail: s_kenji1032@yahoo.co.jp]

Citation: World Neurosurg. (2023) 169:e260-e269. https://doi.org/10.1016/j.wneu.2022.10.121

*Journal homepage: **www.journals.elsevier.com/world-neurosurgery***

*Available online: **www.sciencedirect.com***

residual nidus during or at the end of AVM surgery.[1] Flow 800 (Carl Zeiss, Oberkochen, Germany) analysis obtained after ICG videoangiography increases the ability to more easily understand the available information.[1] However, this technique cannot detect angioarchitecture covered by brain tissue and cannot be used for preoperative planning.

The usefulness of 3-dimensional (3D) multimodal fusion images in AVM surgery for the comprehension of complex angioarchitectures has been reported.[3-8] With transparent images of each structure, 3D multimodal fusion imaging can visualize deep feeders and nidi covered by brain tissue. With 3D information of all the surrounding anatomical structures, useful presurgical simulations can also be created to depict the relationship between a nidus and adjacent cortex. However, 3D multimodal fusion imaging with magnetic resonance angiography or computed tomography angiography is not exact enough due to the limited spatial resolution. Even with 3D rotational angiography (3DRA), 3D multimodal fusion images cannot always clearly visualize all the small feeders and drainers due to the limited temporal resolution, poor source images, and processing techniques.

Utilizing both 3D multimodal fusion images and intra-arterial ICG videoangiography to compensate for the disadvantages of each modality may thus offer an optimal tool for AVM surgery. However, no reports have evaluated the utility of utilizing these 2 techniques for AVM surgery. This study presents the results of utilizing both 3D multimodal fusion images and intra-arterial ICG videoangiography in a series of cerebral AVM surgeries. This report also discusses the efficacy of using these particular techniques.

METHODS

Patient Population

This study was approved by the Clinical Research Review Board at our institution and conducted in compliance with the Health Insurance Portability and Accountability Act regulations. All patients provided written informed consent. This study included 12 consecutive patients with cerebral or cerebellar AVM who underwent preoperative planning with 3D multimodal fusion imaging and ICG videoangiography via intra-arterial injection during surgery from 2018 to 2021. Table 1 summarizes the patient characteristics.

Image Acquisition

Magnetic resonance imaging (MRI) was performed on a 3.0-T system for the head (Discovery MR 750; GE Healthcare, Milwaukee, Wisconsin, USA). T1-weighted imaging (T1WI) with spoiled gradient echo (SPGR) was acquired with an 8-channel phased-array head coil. Imaging sequences and parameters for T1WI with SPGR were: 1) field of view, 240 mm; 2) matrix, 256 × 256; 3) repetition time, 7.7 ms; 4) echo time, 3.0 ms; 5) flip angle, 8°; 6) and slice thickness, 0.9 mm. Computed tomography (CT) was performed using a 320-detector row CT scanner (Aquilion ONE; Canon Medical System, Tokyo, Japan). Slice thickness was 1 mm. A clinical C-arm angiography unit (Allura Clarity FD20/20; Philips Medical System, Best, the Netherlands) was used for 3DRA. The C-arm rotated through 240° at 48°/s and obtained 122 images with a 19-inch field of view during contrast injection. Rotation was initially performed without contrast agent injection to obtain the

Table 1. Characteristics of Patients with Arteriovenous Malformation and Summary of Predissection Assessments of 3-Dimensional Multimodal Fusion Image and Intra-arterial Indocyanine Green Videoangiography

						Qualitative Assessment of Intraoperative Identification			
						Superficial Feeders		Range of Nidus	
Case	Age (years)/Sex	S–M Grade	Location	Size of Nidus (cm)	Number of Feeders	3D Multimodal Fusion Image	IA ICG Video Angiography	3D Multimodal Fusion Image	IA ICG Video Angiography
1	42/M	I	frontal	1	4	I	I	I	III
2	56/M	II	frontal	1	5	I	I	I	III
3	43/F	III	parietal	4	11	II	I	I	III
4	15/M	III	occipital	2.5	3	I	I	I	III
5	23/F	V	frontal	6.5	15	II	I	I	III
6	69/F	I	cerebellum	2	6	III	I	I	III
7	50/M	I	frontal	1	1	I	I	I	I
8	47/M	III	parietal	4	5	I	I	I	III
9	52/M	III	parietal	4	11	II	I	I	III
10	70/F	I	frontal	1	3	I	I	I	III
11	68/F	I	cerebellum	2	7	III	I	I	III
12	10/M	III	occipital	4	6	I	I	I	III

S-M grade, Spetzler–Martin grade; IA, intra-arterial; ICG, indocyanine green; M, male; F, female.

bone image, after which rotation was performed with contrast injection. The 3DRA was performed in the arterial phase (X-ray delay, 2.5–3 seconds) and venous phase (X-ray delay, 7–8 seconds). The volume and injection rate of contrast agent were 15 ml and 3 ml/s for the internal carotid artery, and 12.5 ml and 2.5 ml/second for the vertebral artery, respectively. Reconstruction of 3D volume data was performed with a matrix size of 384 × 384 × 384.

Image Processing

All data were provided as image stacks coded in Digital Imaging and Communications in Medicine format and processed with Synapse Vincent (Fujifilm, Tokyo, Japan) for 3D multimodal fusion image reconstruction. Imaging data from MRI, CT, and 3DRA were fused automatically with the normalized mutual information method. The modality/sequence offering the highest contrast of the target tissue was selected for 3D modeling of the tissue. Bone tissue images were extracted from CT data. Normal brain tissue images were extracted from T1WI with SPGR data. If MRI was unavailable, normal brain tissue images were extracted from CT. Vessel images were extracted from 3DRA data. Vein images were extracted from 3DRA performed during the late venous phase. The 3D model was constructed using volume-rendering methods. Manual segmentation was used to distinguish small anatomical structures, such as feeder vessels, normal arteries, and veins, from surrounding noise. Preoperative analysis of the relationship between feeders, nidi, drainers, and surrounding normal cerebral tissues was performed using 3D multimodal fusion images. Normal cerebral tissues were made transparent on 3D multimodal fusion images to investigate the underlying feeders and nidi.

Intra-Arterial Injection for ICG Videoangiography

ICG videoangiography studies were performed using either the OPMI Pentero or Kinevo with integrated ICG technology (Carl Zeiss, Oberkochen, Germany) in a previously reported method.[1] Intraoperative DSA was routinely performed in our hybrid operating room that was used for AVM surgeries. After general anesthesia, a 5-Fr sheath was inserted into the right femoral artery. A heparin-coated 5-Fr catheter was then introduced into the carotid artery or vertebral artery. The intraoperative DSA study was primarily performed before dissection and after total dissection of the AVM. In addition to the intraoperative DSA procedure, 5 ml of ICG (a 2.5-mg dose dissolved in 50 ml of heparinized saline; 4 U/ml) was injected through the catheter used for ICG videoangiography. Arterial, capillary, and venous angiographic images were observed in real time on the video screen. Flow 800 software was used to analyze the video obtained during this procedure.

Assessment of Intraoperative Anatomical Findings

An understanding of the anatomical structures of superficial feeders (and drainers) and the range of the nidus is an important first step in AVM surgery. The utility of 3D multimodal fusion images and intra-arterial ICG videoangiography to identify superficial feeders and range of the nidus was assessed by comparing each image and surgical field during surgery. Assessment was performed by the operating surgeons. The utility of each image was assessed qualitatively using the following categories: 1) "Class I", the image visualized ≧80% of all superficial feeders in the surgical field and the range of the nidus as estimated from the image was found to be precise; 2) "Class II", the image visualized <80% of all the superficial feeders in the surgical field; and 3) "Class III", the image was useless for identifying superficial feeders and for estimating the range of the nidus regardless of its visualization.

Table 2. Relationship Between Predissection Assessment and Morphological Features of Arteriovenous Malformation Regarding Intraoperative Identification of Superficial Feeders by 3-Dimensional Multimodal Fusion Imaging

	Class I	Class II	*P*
Mean number of feeders	4	12.3	0.02
Mean size of nidus (cm)	2	4.8	0.08

Statistical Analysis

The Mann-Whitney U test was used to compare nonparametric numerical variables. For all statistical analyses, values of $P < 0.05$ were considered significant. All statistical analyses were performed using the SPSS Statistics version 28 software package (IBM Corporation, Tokyo, Japan).

RESULTS

Of the 12 cases evaluated, intraoperative identification of superficial feeders was "Class I" in all cases by intra-arterial ICG videoangiography, but "Class III" in 2 cerebellar AVM cases by 3D multimodal fusion imaging (Table 1). In the remaining 10 cases of cerebral AVM, results were "Class I" in 7 cases and "Class II" in 3 cases with 3D multimodal fusion images (Table 1). The number of feeders was significantly larger in the "Class II" group than in the "Class I" group, and size of the nidus tended to be larger in the "Class II" group than in the "Class I" group (Table 2). Intraoperative estimation of the range of the nidus, in all cases other than one small, superficial nidus, was "Class III" by ICG videoangiography, but "Class I" by 3D multimodal fusion image in all cases (Table 1). Postoperative angiography showed complete resection of the AVM in all cases with no complications.

Illustrative Cases

Case 8. MRI performed in a 47-year-old man who presented with headache demonstrated an incidental AVM (Figure 1A). In addition, DSA indicated a Spetzler–Martin grade III AVM in the right parietal lobe, fed by the middle cerebral artery and posterior choroidal artery and draining into the vein of Trolard and superficial middle cerebral vein (Figure 1B and C). A 3D multimodal fusion image showed that the nidus was located in the inferior parietal lobule, fed by 4 superficial feeders from the middle cerebral artery and one deep feeder from the posterior choroidal artery (Figure 1D and E). The patient underwent right parietal craniotomy, and the nidus was removed after feeder embolization. Intraoperative identification of superficial feeders was easy from 3D multimodal fusion images (Figure 2A and C). Flow 800 was used to analyze the captured video of intraoperative ICG videoangiography, and this analysis made identification of superficial feeders and drainers even easier

(Figure 2B and C). In addition, fine drainers that were not shown in the 3D multimodal fusion image were revealed (Figure 2A–C; double arrowheads). Although the location of the nidus was easy to identify by Flow 800 analysis, the range of the nidus was difficult to estimate (Figure 2B and C). However, the range of the nidus was able to be estimated from the 3D multimodal fusion image (Figure 2D–F), and the nidus was removed based on the estimated nidus contour (Figure 3A and C). Flow 800 analysis demonstrated the color of drainers as green prior to dissection, changing to blue after dissection, indicating a slowing of nidus flow (Figure 3B and D). After complete dissection of the nidus (Figure 3E), ICG videoangiography demonstrated no filling of either the nidus or the drainers (Figure 3F). Postoperative DSA showed complete resection of the AVM (Figure 3G and H).

Case 11. A 68-year-old woman presented with disturbance of consciousness. CT demonstrated left cerebellar hemorrhage. DSA revealed a Spetzler–Martin grade I AVM in the left cerebellar hemisphere, fed by the left superior cerebellar artery (SCA) and left posterior inferior cerebellar artery (PICA) branching from the common trunk with the anterior inferior cerebellar artery and draining into the jugular vein through the petrosal vein, superior petrosal sinus, cavernous sinus, and inferior petrosal sinus (Figure 4A–D). Urgent suboccipital decompressive craniectomy was performed. A 3D multimodal fusion image showed the

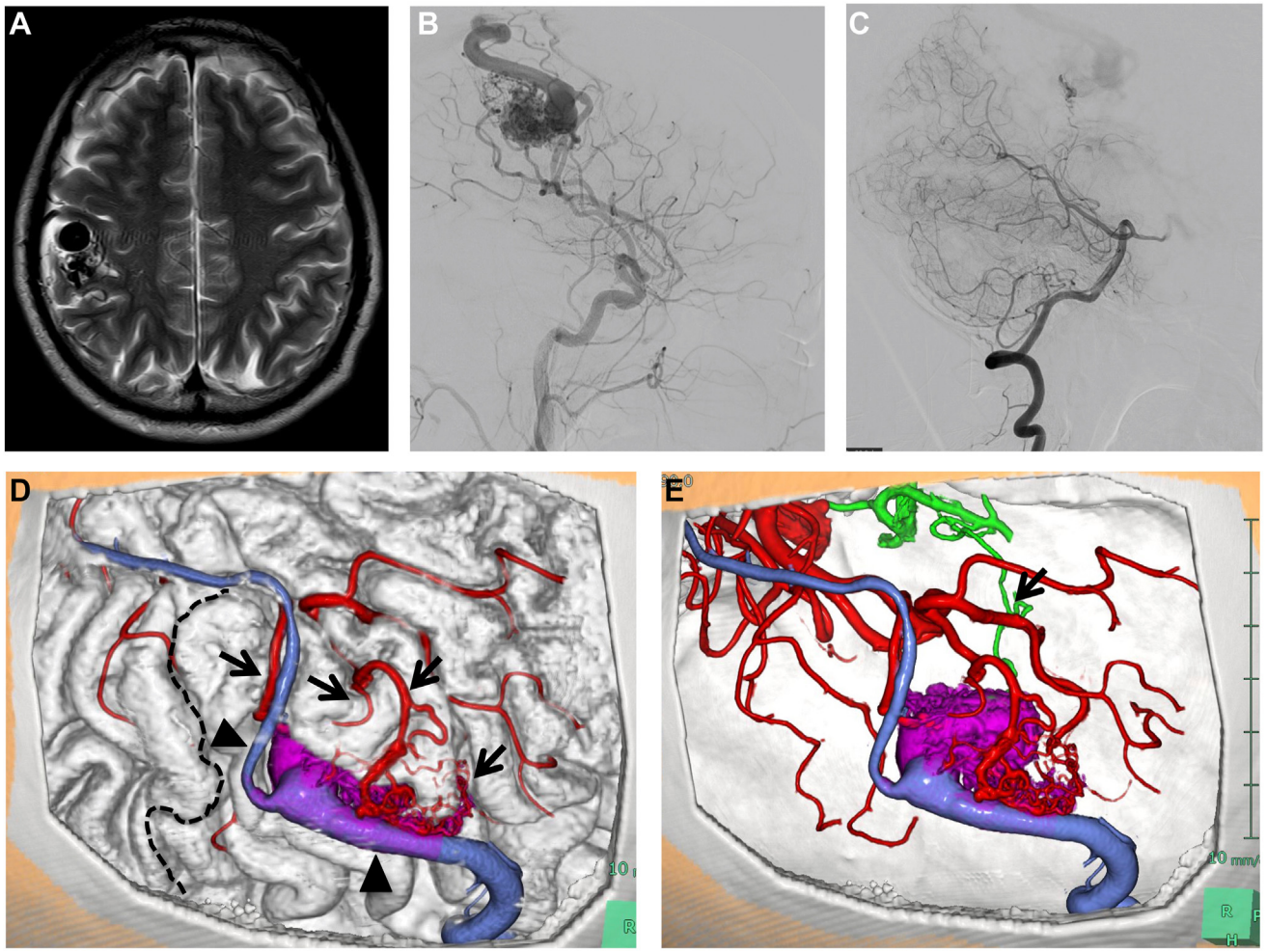

Figure 1. Case 8. (**A**) Magnetic resonance imaging shows an arteriovenous malformation (AVM) in the right parietal lobe. (**B**) Lateral-view right internal carotid angiography reveals that the AVM is fed by the middle cerebral artery and drains into the vein of Trolard and superficial middle cerebral vein. (**C**) Lateral-view right vertebral angiography shows that the AVM is fed by the posterior choroidal artery. A 3D multimodal fusion image shows that the nidus is located in the inferior parietal lobule and fed by 4 superficial feeders from the middle cerebral artery (**D**) and one deep feeder from the posterior choroidal artery (**E**). *Dotted line* indicates central sulcus; arrows indicate feeders; arrowheads indicate drainers (**D** and **E**).

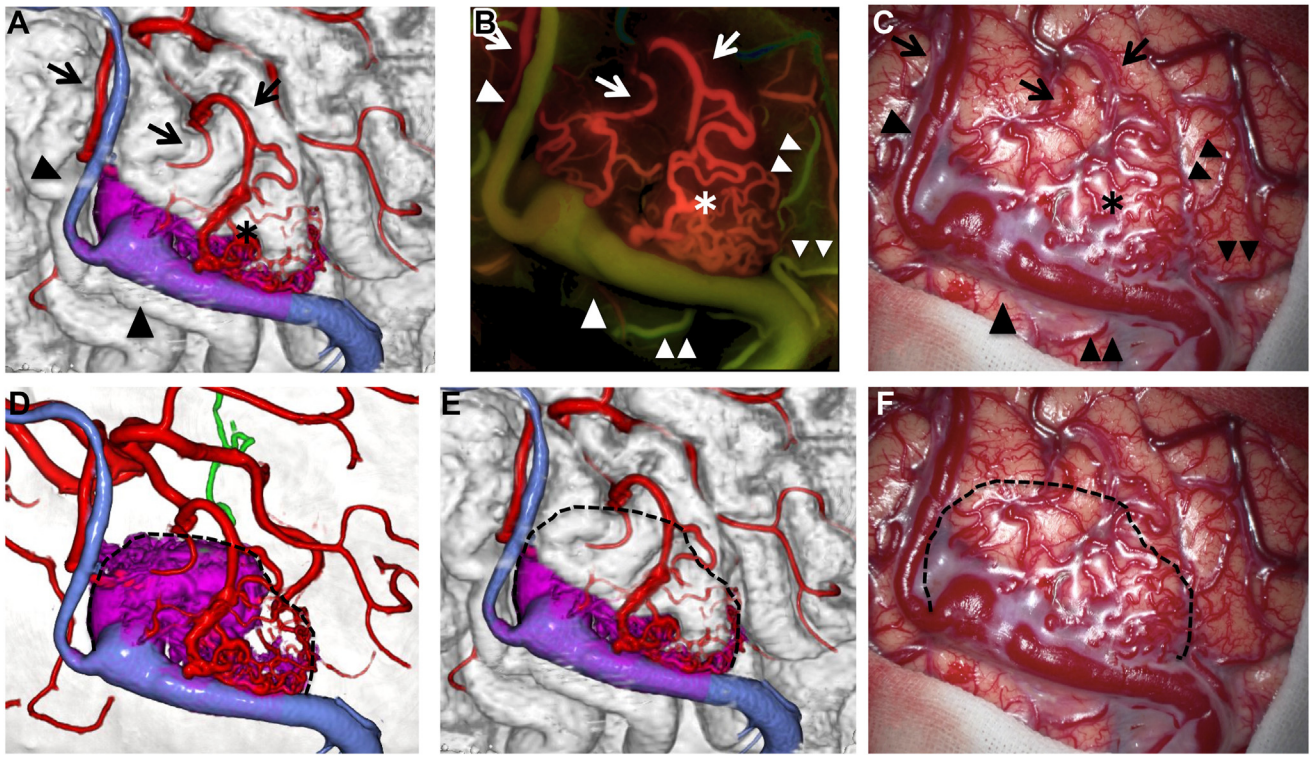

Figure 2. Case 8. A 3-dimensional (3D) multimodal fusion image (**A**), Flow 800 image analyzing indocyanine green (ICG) videoangiography (**B**), and surgical view (**C**) before dissection of the nidus. The 3D multimodal fusion image shows almost the same relationship between superficial feeders, drainers and surrounding structures as the surgical view. Flow 800 analysis provides a more precise figure than 3D multimodal fusion image, including fine feeders and drainers not shown in the 3D multimodal fusion image (*arrows* indicate feeders; asterisk indicates nidus; arrowheads indicates drainers; double arrowheads indicate fine drainers not shown on 3D fusion images). The 3D multimodal fusion image reveals the contours of the nidus (**D**) and the relationships with surrounding structures (**E**). The contour of the nidus was estimated in the operative field referring to the 3D multimodal fusion image (*dotted line* indicates contour of the nidus) (**F**).

nidus located in the left upper cerebellar hemisphere, fed by 3 superficial feeders from the left PICA and deep feeders from the SCA (Figure 4E and F). One month later, the nidus was removed after embolization of the deep feeders from the SCA (Figure 5A). Intra-arterial ICG videoangiography showed the feeders appearing at 1 second, after which the feeders disappeared and normal veins and the transverse sinus (but not the nidus or drainers) appeared at 5 seconds, with normal veins still apparent at 10 seconds (Figure 5B–D). Intraoperative identification of superficial feeders from the 3D multimodal fusion image was difficult due to the fuzzy appearance of cerebellar arteries (Figure 5A and E). However, since the view for ICG videoangiography is the same as that seen during surgery when viewed under a microscope, superficial feeders were easily identified, although the range of the nidus was difficult to estimate (Figure 5A, B and F). Range of the nidus was estimated from a 3D multimodal fusion image (Figure 5G and H) and the nidus was removed according to the estimated nidus contours. After complete dissection of the nidus (Figure 5I), ICG videoangiography showed no filling of either the nidus or drainers (Figure 5J). Postoperative DSA showed complete resection of the AVM (Figure 5K and L).

Case 9. A 52-year-old man presented with visual field defect. CT showed cerebral hemorrhage in the left occipital lobe and DSA revealed a Spetzler–Martin grade III AVM in the left parietal lobe, fed by the anterior and middle cerebral arteries and draining into the vein of Trolard and superficial middle cerebral vein (Figure 6A and B). The patient underwent parietal craniotomy and the nidus was removed after feeder embolization (Figure 6C). Superficial feeders, nidi, and drainers were easily identified by Flow 800 obtained by analyzing ICG videoangiography as well as the 3D multimodal fusion image. However, the 3D multimodal fusion image was not as precise as ICG videoangiography regarding superficial fine feeders adjacent to the main drainer (Figure 6C–E, yellow dotted circle). Although the range of the nidus seemed estimable by Flow 800 analysis (Figure 6D, yellow dotted line), the 3D multimodal fusion image demonstrated a nidus

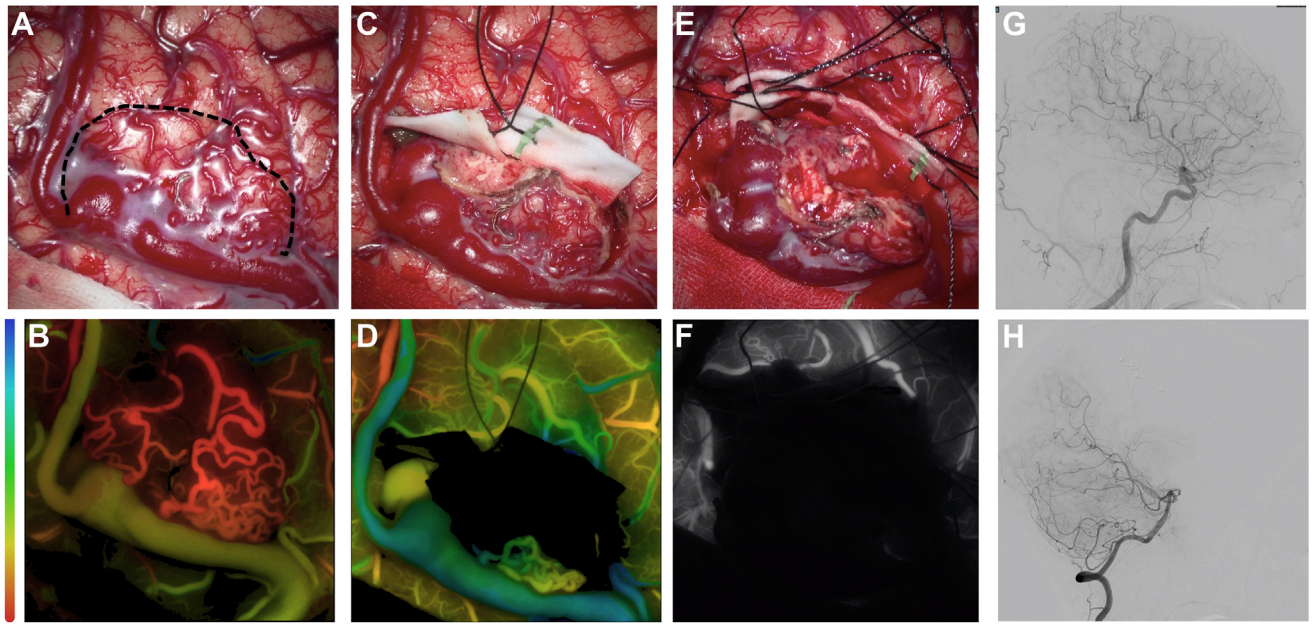

Figure 3. Case 8. Surgical view before dissection (*dotted line* indicates contour of the nidus) (**A**), after dissection according to the estimated contour (**C**), and after complete dissection (**E**) of the nidus, as well as Flow 800 image analyzing ICG videoangiography studies (**B** and **D**) and ICG videoangiography (**F**). Flow 800 analysis demonstrates that the color of drainers is green prior to dissection and changes to blue after dissection, indicating a slowing of nidus flow (**B** and **D**). After complete dissection of the nidus (**E**), ICG videoangiography demonstrates no filling of either the nidus or drainers (**F**). Postoperative lateral view in right internal carotid angiography (**G**) and right vertebral angiography (**H**) shows complete resection of the arteriovenous malformation.

component fed by the anterior cerebral artery, which could not be observed from the cerebral surface (Figure 6F). The nidus was dissected according to the contours estimated by Flow 800 analysis (Figure 7C) at the beginning. Flow 800 analysis after dissection according to the estimated contours demonstrated that the color of the main drainer did not change much compared with that before dissection of the nidus, indicating little reduction in nidus flow (Figure 7B–D). Nidus dissection was therefore extended to the contours as estimated by the 3D multimodal fusion image (Figure 7E). ICG videoangiography demonstrated no filling of either the nidus or drainers after complete dissection of the nidus range estimated from the 3D multimodal fusion image (Figure 7F).

DISCUSSION

This is the first study to demonstrate that utilizing both 3D multimodal fusion images and intra-arterial ICG videoangiography in AVM surgery can be useful for identifying superficial feeders and estimating the range of the nidus, as compared to that using either 3D multimodal fusion images or intra-arterial ICG videoangiography alone. The greater the number of feeders, the more difficult the task of precisely identifying the vascular anatomy from 3D multimodal fusion images is. Since superficial arteries of the cerebellum appeared fuzzy, identifying superficial feeders from 3D multimodal fusion images was also difficult. However, the number and location of feeders did not affect understanding the superficial vascular anatomy by intra-arterial ICG videoangiography. A previous study showed that intra-arterial ICG videoangiography was useful to identify the nidus location,[1] but not to identify the precise range of the nidus. However, identifying the precise range of the nidus from the 3D multimodal fusion image was helpful. The nidus was therefore resected according to contours estimated from 3D multimodal fusion images. Flow 800 analysis obtained after intra-arterial ICG videoangiography demonstrated flow dynamic changes of the nidus during dissection. This kind of information cannot be obtained from 3D multimodal fusion images.

A key disadvantage of intra-arterial ICG videoangiography is that feeders or nidi covered by brain tissue cannot be detected. However, 3D multimodal fusion images can provide transparent images of each structure and detect deep feeders and nidi under the cerebral surface. Moreover, 3D multimodal fusion images could visualize the vascular anatomy and surrounding structures (e.g., central sulcus) preoperatively, providing useful information when planning embolization or approaches to occlude deep parts of feeders, and in determining the range of nidus resection in consideration of the relationship between the nidus and adjacent

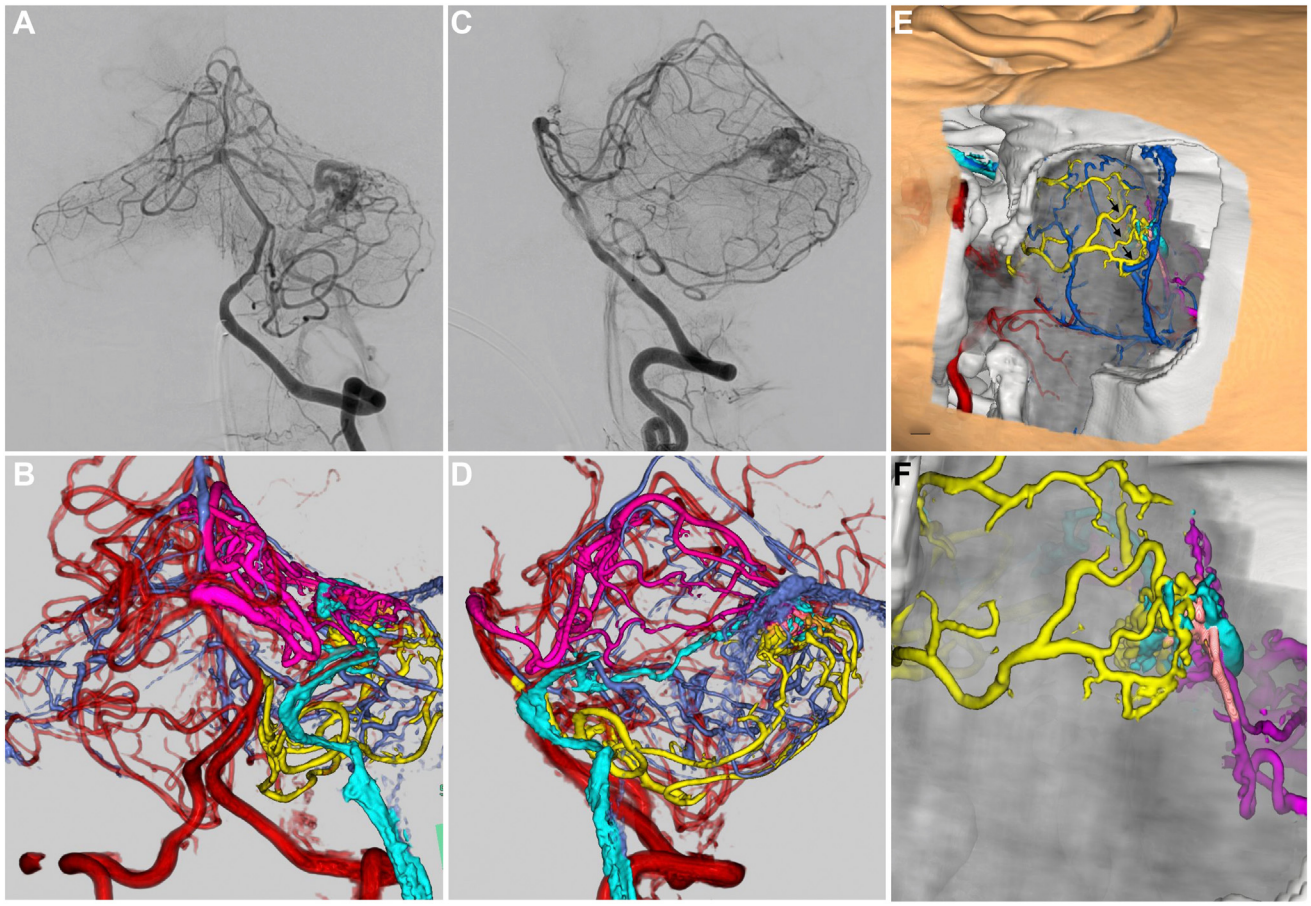

Figure 4. Case 11. Anteroposterior (AP) (**A**) and lateral (**C**) view of left vertebral angiography, and AP (**B**) and lateral (**D**) view of 3D rotational angiography show an arteriovenous malformation fed by the left superior cerebellar artery (SCA) and left posterior inferior cerebellar artery (PICA) branching from the common trunk with the anterior inferior cerebellar artery and draining into the jugular vein through the petrosal vein, superior petrosal sinus, cavernous sinus, and inferior petrosal sinus. A 3D multimodal fusion image of the operative view shows the nidus located in the left upper cerebellar hemisphere and fed by 3 superficial feeders from the left PICA (*arrows* indicate superficial feeders) (**E**). Magnified view of the 3D multimodal fusion image reveals deep feeders from the SCA (**F**). *Pink color* indicates SCA in panels B, D, E, and F. *Yellow color* indicates PICA in panels B, D, E, and F. Cyan color indicates the drainer in panels B, D, E, and F. Blue color indicates normal veins and venous sinus in panels B, D, and E.

cortex. In our institution, 3D multimodal fusion images can be utilized in the operating room during AVM surgery using a mobile PC containing 3D multimodal fusion image data. The 3D fusion image can be moved freely on the screen, providing any surgical view the operator desires, from superficial to deep parts by providing transparent images from every direction. The 3D multimodal fusion image thus compensates for the various disadvantages of intra-arterial ICG videoangiography.

In AVM surgery, neither intravenous nor intra-arterial ICG videoangiography can usually detect feeders or drainers covered by brain tissue. Only intraoperative DSA can visualize all the feeders, nidi, and drainers, but this modality is markedly inferior to intra-arterial ICG videoangiography in terms of simplicity, speed, and spatial resolution. Therefore, unlike bypass or aneurysm surgery, we routinely perform intraoperative DSA for AVM surgery in our hybrid operating room to compensate for this disadvantage of ICG videoangiography. Furthermore, we have just added the step of injecting ICG to the contrast medium administered through the catheter. Intra-arterial ICG videoangiography is therefore easily performed in any institution that routinely performs intraoperative DSA for AVM surgeries. However, image-processing techniques for 3D multimodal fusion images are time-consuming, since this requires manual segmentation of each vessel by differentiating between feeders, drainers, and normal vessels. Regarding AVMs, information on the vascular anatomy is the most important and was obtained from 3DRA. However, since 3DRA does not contain a temporal dimension, differentiation of feeders, nidi, drainers, and normal vessels cannot be performed automatically.

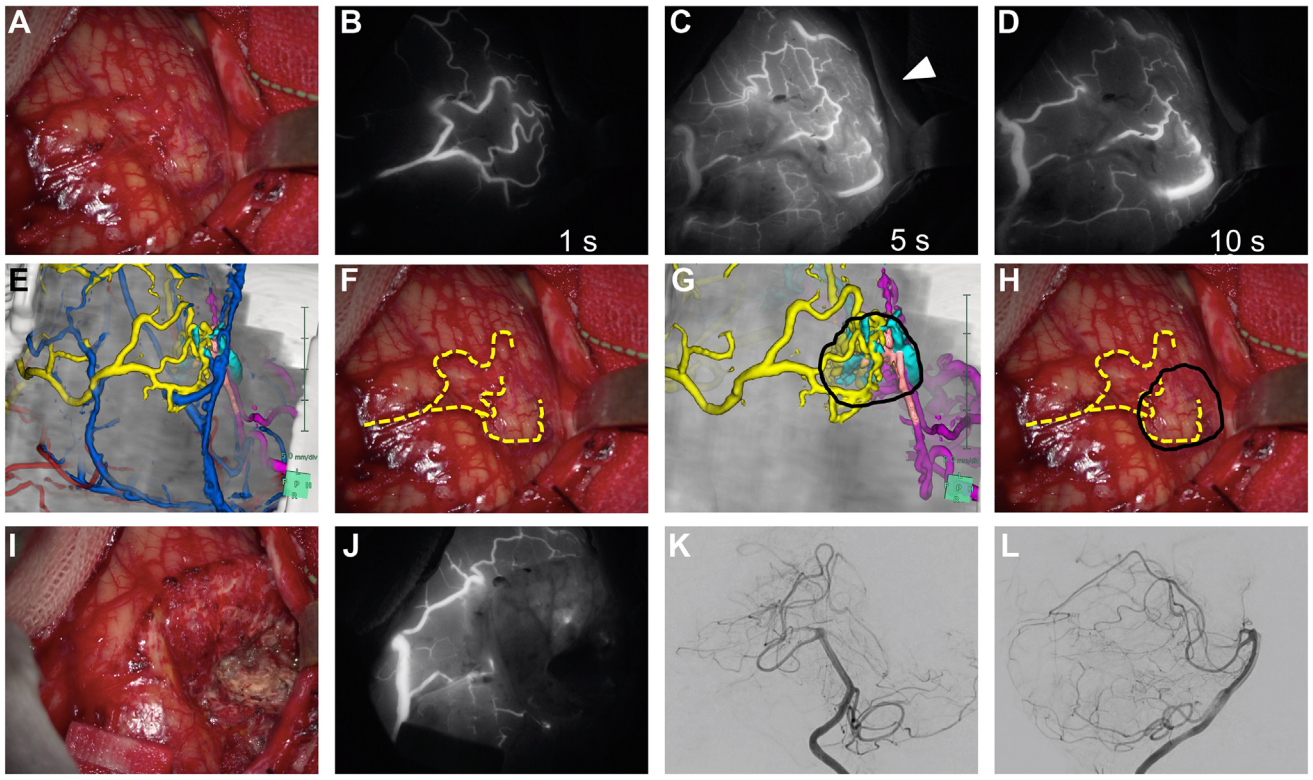

Figure 5. Case 11. Surgical views (**A**, **F**, **H**), and ICG videoangiography studies (**B**, **C**, **D**) before dissection of the nidus. Intra-arterial ICG videoangiography shows that the feeders appear at 1 second, after which the feeders disappear, and normal veins and transverse sinus, but not nidus and drainers, appeared at 5 seconds, with normal veins still appearing at 10 seconds (*arrowhead* indicates transverse sinus) (**C**). Intraoperative identification of superficial feeders by 3D multimodal fusion images (**E** and **A**) is difficult due to fuzzy appearance of the cerebellar arteries. However, since the ICG videoangiography view (**B**) is the same as that seen during surgery when viewed under a microscope, identifying superficial feeders (*yellow* dotted lines indicate feeders from PICA) (**F**) is easy, while estimating the range of the nidus is difficult. A 3D multimodal fusion image reveals contours of the nidus (circle indicates contour of the nidus) (**G**). The contour of the nidus is estimated in the operative field with reference to the 3D multimodal fusion image (H: yellow dotted lines indicate feeders from PICA; circle indicates contour of the nidus). After complete dissection of the nidus (**I**), ICG videoangiography demonstrated no filling of either the nidus or drainers (**J**). Postoperative anteroposterior (**K**) and lateral (**L**) views of the left vertebral angiography show complete resection of the arteriovenous malformation.

Differentiation of these vessels depends on the creator's understanding of the vascular anatomy, which might lead to the introduction of bias into the 3D multimodal fusion image. The quality of 3D multimodal fusion images also depends on the status of the source images for each modality. Not all feeders are visualized on 3DRA owing to factors such as imaging timing, motion artifacts, and small vessels. However, intra-arterial ICG videoangiography contains a temporal dimension with high phase contrast. Flow 800 analysis of color-encoded blood flow images is also information containing a temporal factor, facilitating the differentiation of feeders, drainers, and normal vessels. In addition, intra-arterial ICG videoangiography visualized the entire vascular anatomy of the surgical field containing small, fine, and fuzzy vessels. Intra-arterial ICG videoangiography thus compensates for the various disadvantages of 3D multimodal fusion images.

Previous reports have described the utility of 3D multimodal fusion image techniques for AVM surgical simulation.[3-8] Although some authors used only MR angiography and MR venography as vessel images, the spatial resolution for each vessel is not as high as 3DRA.[3,5] A recent study reported the development of 3D multimodal fusion image techniques using 3DRA or 4D DSA as a source of vessel images to visualize the precise morphology of AVMs and differentiated feeders, nidi, drainers, and normal vessels preoperatively.[4,6-8] However, as we mentioned, the 3D multimodal fusion image technique is time-consuming and contains some bias from the creator. In addition, source images from 3DRA cannot always visualize all vessels due to the lack of a temporal dimension and the presence of motion artifacts. Intra-arterial ICG videoangiography visualizes all superficial vessels with a temporal factor, and also shows flow direction in vessels and flow dynamic changes

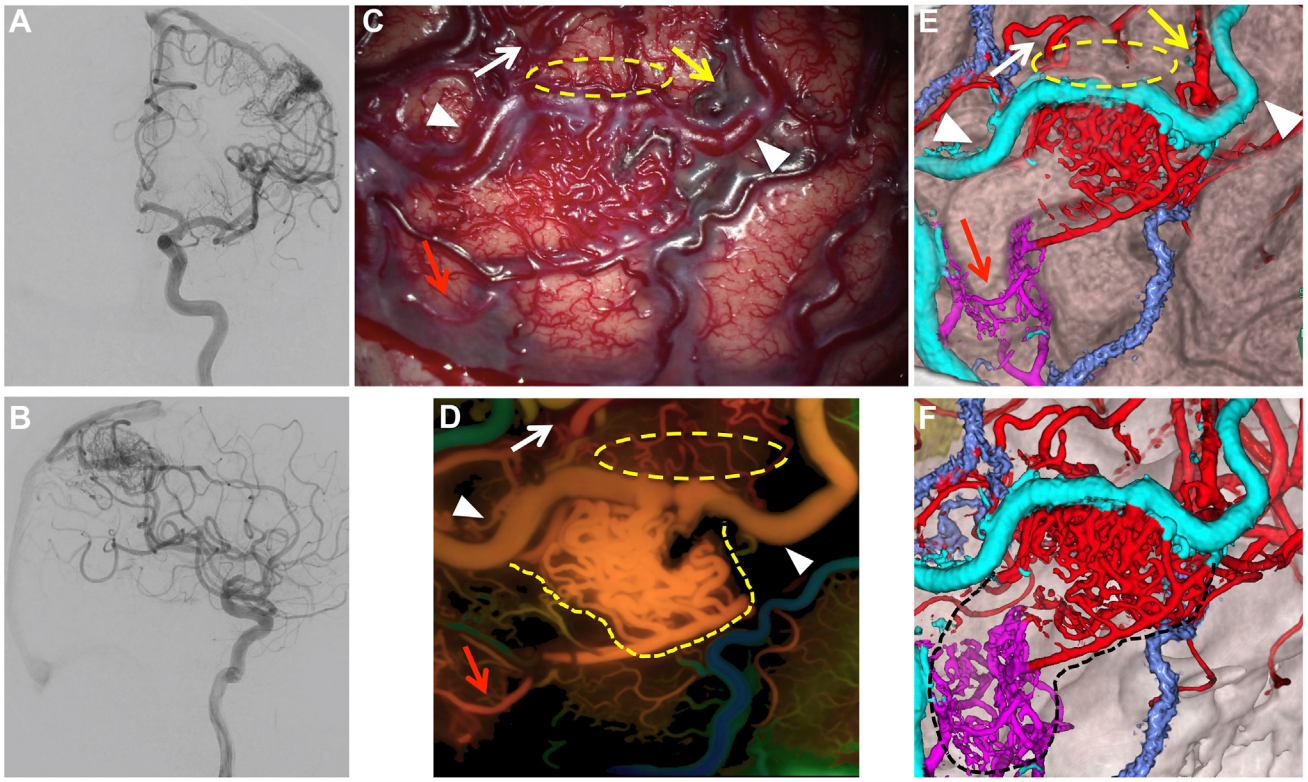

Figure 6. Case 9. AP (**A**) and lateral (**B**) views of the left internal carotid angiography reveal an arteriovenous malformation fed by the anterior cerebral artery and middle cerebral artery and draining into the vein of Trolard and superficial middle cerebral vein. Surgical view (**C**), Flow 800 image analyzing ICG videoangiography (**D**) and 3D multimodal fusion image (**E** and **F**) before dissection of the nidus. Superficial feeders, nidus, and drainers are easily identified by the Flow 800 obtained by analyzing ICG videoangiography as well as 3D multimodal fusion images (**E**). However, 3D multimodal fusion images are not as precise as ICG videoangiography regarding superficial fine feeders adjacent to the main drainer (*white arrow* indicates feeder from the middle cerebral artery; red arrow indicates feeder from the anterior cerebral artery; *yellow arrow* indicates feeder occluded by presurgical embolization; arrowheads indicate drainers; yellow dotted circle indicate fine feeders not shown in the 3D multimodal fusion image; yellow dotted line indicates estimated contour of the nidus). The 3D multimodal fusion image demonstrates the nidus component fed by the anterior cerebral artery, which could not be observed from the surface of the cerebrum (F: *black dotted* circle indicates the estimated contour of the nidus).

of the nidus without a time-consuming procedure, compensating for the disadvantages of 3D multimodal fusion images. The utilization of both techniques for AVM surgery is thus more useful and safer than using either technique alone.

Some limitations to this study must be considered. The sample size was small, and this was not a comparative study (such as a comparison of combination use vs. single use), so accumulation of further data and cases along with comparisons to other modalities will be necessary to definitively evaluate the safety and efficacy of this technique.

CONCLUSIONS

Utilizing both a 3D multimodal fusion image and intra-arterial ICG videoangiography is more useful than single use of each method alone in AVM surgery, especially for identifying superficial feeders and estimating the range of the nidus. The utility of this technique is attributable to each method compensating for the disadvantages of the other. Our technique is thus expected to offer a very helpful support tool in AVM surgery.

CRediT AUTHORSHIP CONTRIBUTION STATEMENT

Kenji Shimada: Conceptualization, Methodology, Writing – original draft. **Kazuhisa Miyake:** Data curation. **Izumi Yamaguchi:** Data curation. **Shu Sogabe:** Data curation. **Masaaki Korai:** Data curation. **Yasuhisa Kanematsu:** Data curation. **Yasushi Takagi:** Supervision.

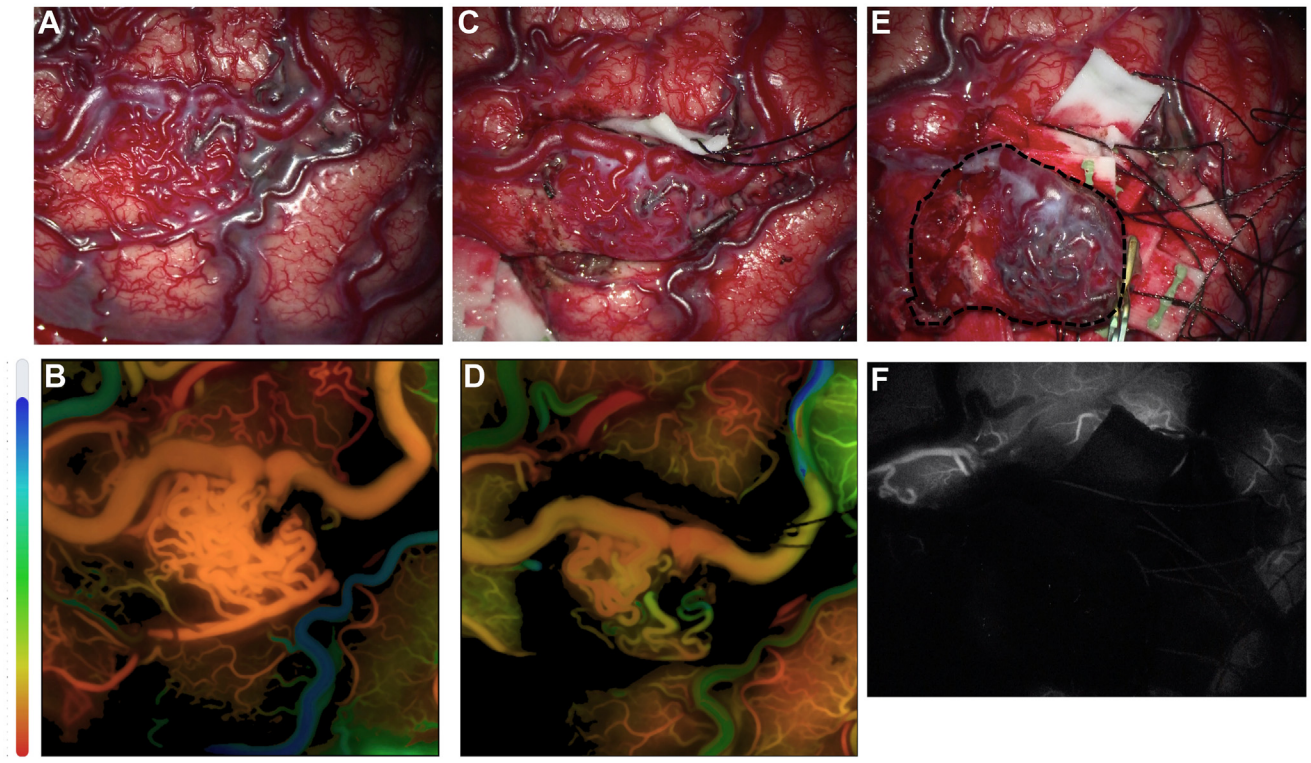

Figure 7. Case 9. Surgical view before dissection (**A**), after dissection according to the contour estimated by Flow 800 analysis (**C**), and after complete dissection according to the contour estimated by 3D multimodal fusion image (**E**), as well as Flow 800 images analyzing ICG videoangiography (**B** and **D**) and ICG videoangiography (**F**). The Flow 800 analysis (**D**) after dissection according to the contour estimated by Flow 800 analysis demonstrates that the color of the main drainer does not change much compared to that (**B**) before dissection of the nidus, indicating little reduction in nidus flow. Nidus dissection is extended to the contour estimated by 3D multimodal fusion image (E: *dotted line* indicates dissected line). ICG videoangiography demonstrates no filling of either the nidus or drainer after complete dissection of the nidus contour as estimated by 3D multimodal fusion image (**F**).

REFERENCES

1. Shimada K, Yamaguchi T, Miyamoto T, et al. Efficacy of intraarterial superselective indocyanine green videoangiography in cerebral arteriovenous malformation surgery in a hybrid operating room. *J Neurosurg*. 2020;134:1544-1552.

2. Shimada K, Yamamoto Y, Miyamoto T, et al. Efficacy of intra-arterial indocyanine green videoangiography in hemangioblastoma surgery: a case report. *NMC Case Rep J*. 2021;8:295-300.

3. Bekelis K, Missios S, Desai A, Eskey C, Erkmen K. Magnetic resonance imaging/magnetic resonance angiography fusion technique for intraoperative navigation during microsurgical resection of cerebral arteriovenous malformations. *Neurosurg Focus*. 2012;32:E7.

4. Ide S, Hirai T, Morioka M, et al. Usefulness of 3D DSA-MR fusion imaging in the pretreatment evaluation of brain arteriovenous malformations. *Acad Radiol*. 2012;19:1345-1352.

5. Ng I, Hwang PY, Kumar D, Lee CK, Kockro RA, Sitoh YY. Surgical planning for microsurgical excision of cerebral arterio-venous malformations using virtual reality technology. *Acta Neurochir (Wien)*. 2009;151:453-463 [discussion: 463].

6. Suzuki H, Maki H, Taki W. Evaluation of cerebral arteriovenous malformations using image fusion combining three-dimensional digital subtraction angiography with magnetic resonance imaging. *Turk Neurosurg*. 2012;22:341-345.

7. Tritt S, Ommer B, Gehrisch S, et al. Optimization of the surgical approach in AVMs using MRI and 4D DSA fusion technique: a technical note. *Clin Neuroradiol*. 2017;27:443-450.

8. Yoshino M, Kin T, Hara T. Usefulness of high-resolution three-dimensional multifusion medical imaging for preoperative planning in patients with cerebral arteriovenous malformation. *World Neurosurg*. 2019;124:e755-e763, 30677580.

Conflict of interest statement: The authors declare that the article content was composed in the absence of any commercial or financial relationships that could be construed as a potential conflict of interest.

Received 27 October 2022; accepted 30 October 2022

Citation: World Neurosurg. (2023) 169:e260-e269.
https://doi.org/10.1016/j.wneu.2022.10.121

Journal homepage: ***www.journals.elsevier.com/world-neurosurgery***

Available online: ***www.sciencedirect.com***